Preprint Submitted to Journal of Mechanical Science & Technology

Performance assessment limits in transonic 3D turbine stage blade rows using a mixing-plane approach †

José C. Páscoa[1,*] Carlos Xisto[1] and Emil Göttlich[2]

[1]*Faculty of Engineering, University of Beira Interior, Covilhã, 6201-001, Portugal*
[2]*Institute for Thermal Turbomachinery and Machine Dynamics, Graz University of Technology, Graz, Styria A-8010, Austria*

Abstract

Numerical computation of gas turbine flowfields demands high computing power. In the present work, we present a detailed analysis of 3D computations for a highly loaded transonic blade and for a gas turbine stage. Comparison between experimental results and numerical computations reveals the precision limits of current modeling assumptions. Computations are performed using a time-marching approach coupled with a mixing-plane model for the exchange of flowfields between stator and rotor domains. Eddy viscosity turbulence models are applied to compute the flow with and without wall functions. Limitations in performance assessment are presented regarding the level of detail used for the geometry definition, the mixing-plane approach, and the near wall turbulence model employed.

Keywords: Turbulence model; Turbine stage; Mixing-plane; Transonic flow

---

1. Introduction

The current practice in gas turbine design industry follows a well-established chain of levels of detail. A master design team establishes the main parameters for the turbomachine. This requires defining the overall pressure ratio, the number of stages, and other main design variables for the gas turbine. This main team is further subdivided into the compressor, turbine, and combustion chamber design teams. For each of these design sub-teams, the level of detail becomes increasingly complex, both in terms of geometry definition and on the quality of physical models used for computations that aim to characterize the flowfield [1].

It is therefore important to upgrade the level of detail in the tools used for design in relation to the several design sub-teams. This should take into consideration both the levels of refinement used to define the geometry and accuracy of the employed numerical model as a function of the increasingly available computing power. Furthermore, the amount of information tackled by the designers, a concern that has always been less focused on, should not delay the design process more than what is necessarily required.

In this study, we concentrated on the turbine stage, and we reserved the intricate work of defining the complex engine geometry to the skilled company designers. Although (CFD) modeling has been applied increasingly in the industry, the accuracy limitations and performance assessment in 3D turbine stages still require computation of benchmark test cases. It is expected that these could distinguish the influence of several assumptions when modeling this class of flows [2].

The analysis of the flow in turbine blades has been extended from 2D to 3D and from pure Euler equations to Navier-Stokes modeling, including for the turbulent flow, thus ensuring improved levels of detail. This has only been made possible due to the fast development of computer power. Initially, most of the flow analyses had been conducted for isolated blade rows. However, this approach was not accurate in many circumstances due to strong coupling and interaction between several blade rows. Another level of detail attained by the numerical methods is the incorporation of moist air effects for steam turbines or for gas turbines in high and wet environments [3]. Aside from internal gas dynamics, combustor performance has been studied as well [4].

For the computation of the interacting blade rows, several approaches can be employed, such as the steady mixing-plane approach or the pseudo-unsteady average passage equations of Adamczyk, or even the application of pure unsteady solution procedure through one blade pitch [5]. To ensure rotor-stator interaction, a 3D unsteady Navier-Stokes analysis is required. However, such an analysis is highly CPU-intensive and expensive in terms of computing power to be regularly used as design procedure, especially in inverse design [6, 7]. Herein,

---

[*] Corresponding author. Tel.: +351 275 329 925, Fax: +351 275 329 972
E-mail address: pascoa@ubi.pt.

we restricted our approach to the mixing plane model.

The mixing plane approach is applied at the blade row interface between the stator-rotor; it can be applied as well to several stages in series. In this approach, it is assumed that the flow is totally mixed and axis-symmetric between the blade rows. This approach can only approximate the effects of radial variation; it cannot account any circumferential variations, such as those created by wakes, leakage, or secondary flows. Nevertheless, it is important to clarify if the pitchwise averaging has not affected the spanwise variation in the flow. In practical applications, the spanwise variations of pressure, velocity, and flow angle, among others, in all of the stations between the hub and tip are obtained from the full 3D Navier-Stokes computation.

Another restriction related to the multiple levels of detail deals with the inclusion of viscous effects into 3D blade row computations. Undoubtedly, this is restricted by the availability of adequate turbulence models. Computations using DNS, or even LES, remain costly in terms of computer resources. The current industrial state-of-the-art approach is also limited in terms of the use of turbulence models vis-à-vis available computing power, the use of wall functions, and the use of low Reynolds turbulence model (i.e., under better circumstances) to resolve fully the boundary layer [8]. Numerical modeling of turbulent flow in turbine blades has been the subject of intensive research. In recent years, special attention was accorded to turbulence modeling [9]. Excellent results were obtained even with the Baldwin-Lomax algebraic model, particularly for low inlet turbulence intensities (i.e., $Tu<0.2$). Generally, only two equation methods are recommended, $k-\omega$ and a low-Re version of $k-\varepsilon$, to model the influence of higher turbulence levels. Most methods predict higher levels of turbulence around the leading edge. This excessive production of turbulence is caused by the high normal strains computed in the stagnation region [2]. Nevertheless, almost all methods can predict the flow in the pressure surface with good accuracy. Another region of interest is the trailing edge. In this region, turbulence methods tend to capture the separation point with oscillations found therein. All algebraic methods achieve undesirable results in the trailing edge region. These methods lack accuracy when big regions of separated flows, shocks, or high inlet turbulence exist. Our approach uses transport models, as this can partly solve this problem [10].

At present, the flow computation for a single blade row can be performed routinely by using a low-Re turbulence model, even with the aid of desktop computers. However, while it can obtain detailed analysis, this approach is inapplicable for iterative designs. The computation of a whole stage is much more demanding in terms of computing resources, and this can only be accomplished typically with the use of wall functions. This gap is dealt with by the current work; that is, to analyze performance assessment limitations under mixing-plane and wall functions assumptions in order to achieve realistic turbine stage computations.

Two experimental benchmark test cases were computed in relation to the present work. One of these test cases was experimentally tested by one of the co-authors [11] at the Institute for Thermal Turbomachinery and Machine Dynamics, Graz University of Technology. First, the flow for the T106 turbine cascade of blades was computed. This was performed using wall functions and by fully resolving the boundary layer [12]. This allowed us to analyze the capabilities of both near wall models using several turbulence closures beyond the mixing-plane assumption. Afterwards, the flow for a transonic turbine stage was computed. For the test case, the mixing-plane limitations were addressed, including the problems associated with a transonic trailing edge that impinges the mixing-plane and hinders computations.

2. Computation of turbulent flow

FLUENT® code was employed for the flow computation. The code can solve the full 3D Navier-Stokes equations through explicit discretization and by employing a time-marching approach. Subsequently, this would be implemented through a three-stage Runge-Kutta integration scheme. A second order upwind discretization in space was retained. For the T106 test case, the mesh comprised both H and O type blocks; for the transonic stage, only H blocks were used.

2.1 Numerical modeling of the T106 cascade

By using the T106 test case, the influence of the near wall model without stator-rotor interaction was computed. This test problem has been used by other authors. Cutrone *et al.* [12] has recently presented new experimental and numerical results.

The inlet flow is subsonic with a Mach number of 0.59. At the inlet, we imposed total pressure, total temperature, and flow angle. At the exit, we imposed static pressure. In order to mimic the results by Cutrone *et al.*, we also imposed 5.8% inlet turbulence intensity with an associated length scale of 2% chord (Fig. 1).

The mesh in Fig. 2 was carefully generated to obtain good smoothness. Consequently, it comprised 20 blocks. For the grid independency studies, two meshes were created, Mesh-A with 1 251 250 nodes and Mesh-B with 30% reduction in the node count, comprising only 466,284 nodes. Both meshes presented an H-type topology except for the O-block around the blade. For Mesh-A, 130 points were distributed around the mirrored half-blade span. In the inter-blade domain, 55 points were used and another 171 nodes were distributed along the axial flow direction. For the latter case, 107 points were distributed along the blade surface. In the B-Mesh, we distributed 91 points along the blade span, 42 onto the inter-blade region, and 122 onto the axial flow direction with 77 on the blade surface. The aft blade computing domain extended by one blade pitch, while the fore domain extended by $0.875\times pitch$. The mesh used in the computations without wall functions comprised 1,535,950 nodes with 130 points along the symmetric blade span and 171 points in the axial direction. Then,

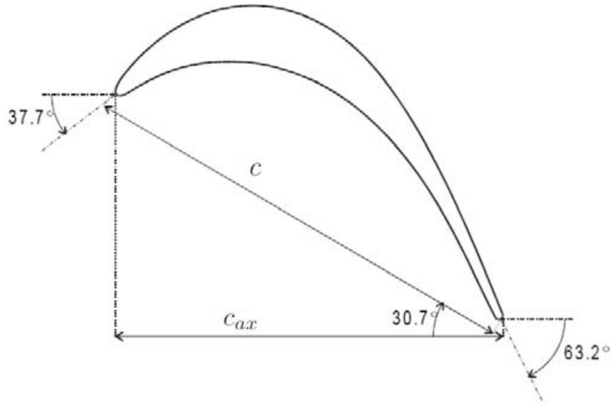

(a)

T106 cascade of blades	
Pitch (*s*)	79.9 *mm*
Chord (*c*)	100 *mm*
Axial chord (c_{ax})	86.1 *mm*
Inlet angle	37.7º
Outlet angle	63.2º
Span	300 *mm*

(b)

Fig. 1. (a) Geometry of the T106 rectilinear cascade; (b) details of the blade geometric parameters.

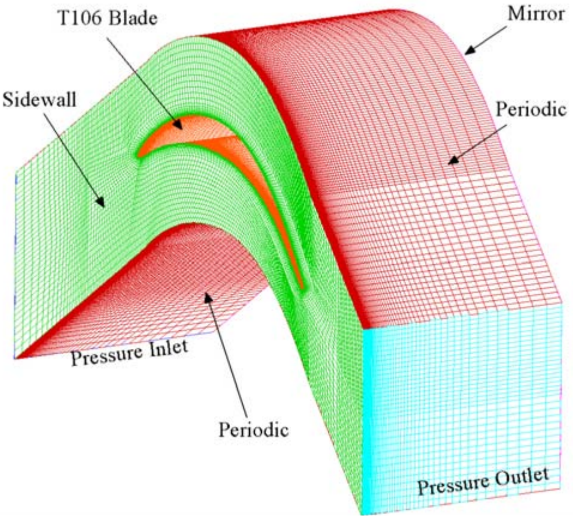

Fig. 2. 3D representation of the mesh with their corresponding boundary conditions.

107 were used to define the blade, and another 65 points were used for the inter-blade region.

2.2 Results obtained for the T106 cascade

Fig. 3 presents the comparison between experimental and numerical results. These were obtained using the high-Re standard $k-\varepsilon$ turbulence model and the Spalart-Allmaras (SA) low-Re turbulence model; both used wall functions (i.e., grid B). The wall function computational model was guaranteed by setting y^+ between 30 and 300. Results from the whole boundary layer were also obtained. These were computed for a y^+ maximum of 0.48 in its spanwise distribution and with a maximum value of 0.53 in the sidewall.

It should be recalled that the boundary layer was modeled by multiple layers when employed for the wall functions. Thus, it comprised a laminar sub-layer, a viscous-turbulent layer, and an outer layer dominated by turbulence. Based on experiments, wall functions can be employed to model this complex near-wall flow structure. Even when $y^+ > 11.63$, the boundary layers are considered turbulent, and thus, we follow the usual practice of maintaining y^+ between 30 and 300. It is generally assumed that y^+ should be pushed back to the lower 30 boundary of the interval when the aim is to ensure a good resolution of the flow gradients. Whenever possible, this was maintained while computing for the results, at least for a major portion of the walls.

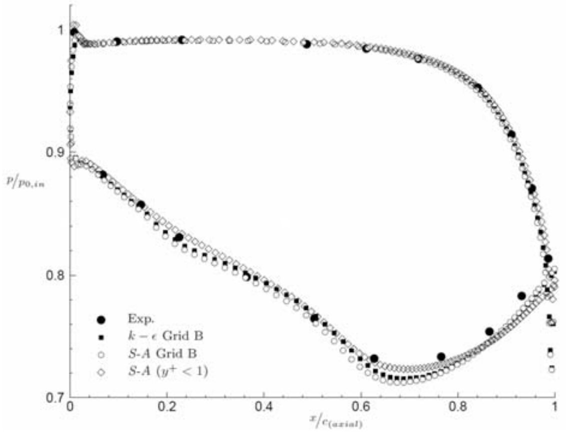

Fig. 3. Comparison between the experimental and computed pressure distributions for the T106 cascade.

Fig. 4 shows the passage vortex computed for the T106 blade using the wall functions. The whole boundary layer using y^+ near 1 was resolved. These results allowed for the assessment of the capability of the wall functions in predicting secondary flows. The intensity of the passage vortex obtained with the models using wall functions was smaller compared with those employing SA to resolve the whole boundary layer.

Results shown in Fig. 4 and Fig. 5 were obtained with the SA turbulence model. Fig. 5 presents the streamlines computed for the T106 blade. The computation utilized the SA turbulence closure with wall functions. Results were also obtained by resolving the whole boundary layer. The plane used to describe the passage vortex, computed in a perpendicular plane to the direction of the flow and placed downstream of the trailing edge, was likewise established.

2.3 Numerical modeling of the transonic turbine stage

The transonic test case was tested experimentally by one of the co-authors at the Institute for Thermal Turbomachinery and Machine Dynamics of Graz Technical University [11]. The test case was representative of state-of-the-art geometries for the last stages of modern gas turbine engines. High level of detail for the geometry was considered, including detailed modeling of the fillets near the hub and tip sections. The stator comprises 24 blades while the rotor had 36 blades, representing a ratio of 2:3 between the stator and rotor blades. In our case, the use of the mixing plane model facilitated the computation, and only one blade was used for the stator and rotor rows.

Table 1. Details on the geometry and flow conditions of the Graz transonic turbine stage.

Stator blade number	24
Rotor blade number	36
Stator chord at mid-span	78.9 mm
Axial stator chord at mid-span	56.1 mm
Stator geometric turning angle	70 °
Rotor chord at mid-span	55.9 mm
Axial rotor chord at mid-span	46.8 mm
Rotor geometric turning angle	107 °
Stator aspect-ratio	0.7
Rotor aspect-ratio	1.24
Pressure-ratio $p_{tot,in} / p_{out}$	3.5
Rotating speed	10 600 rpm
Total pressure, at inlet	403 K
Stator Reynolds number	2.57x10^{6}
Rotor Reynolds number	1.69x10^{6}

The mesh comprised 15 H blocks, with 8 blocks in the stator and 7 in the rotor. The overall mesh comprised 224,136 nodes (131,136 for the stator and 93,000 for the rotor). The stator blade comprised 49 points in the inter-blade region and 93 points in the axial flow direction, with 65 points used to define the blade surface. We distributed 30 points for the radial direction. For the rotor blade, 29 points were applied in the inter-blade zone and 93 on the axial direction, with 65 points used to define the blade geometry. Then, 30 points were used for the radial direction. The mesh is presented in Fig. 6.

2.4 Results obtained for the transonic turbine stage

The first phase of the computations performed for the stage was conducted using isolated blade rows for the stator and rotor. By solving each flow in an isolated blade row, we were able to detect any flow convergence problems typically created by poor mesh quality. This was imperative for a highly complex geometry, particularly because we aimed to model accurately the fillets and rotor gap. After this fine-tuning of the mesh, we proceeded to the full stage computation.

For the test case, we solved the Navier-Stokes equations using the SA turbulence model. This model can perform better in the T106 test case even with wall functions. In this compu-

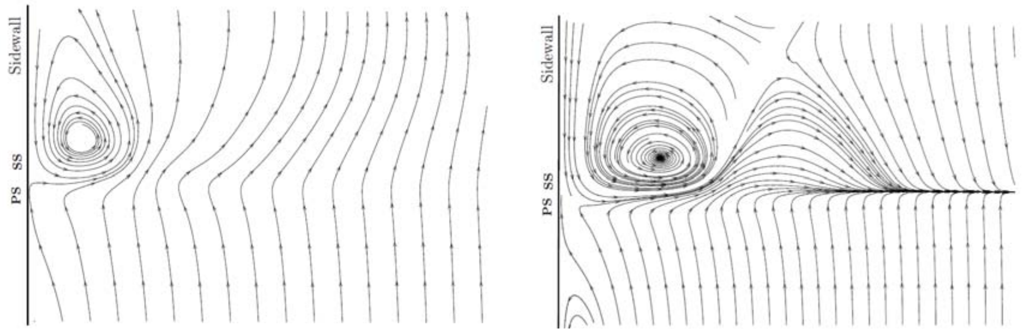

(a) (b)

Fig. 4. Representation of the passage vortex (a) computed for the T106 blade using wall functions and (b) by fully resolving the boundary layer.

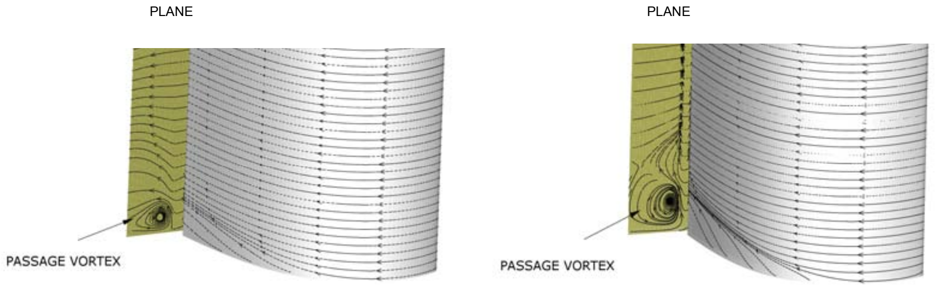

(a) (b)

Fig. 5. Representation of the passage vortex (a) computed for the T106 blade using wall functions and (b) by fully resolving the boundary layer.

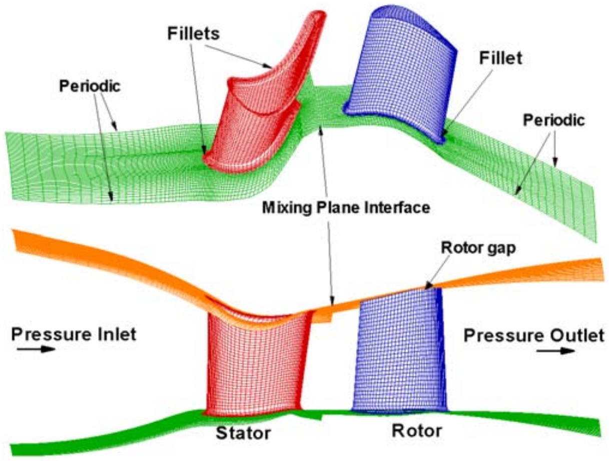

Fig. 6. Mesh used for the computation of the Graz transonic turbine stage. Top image depicts the mesh at the hub surface. Bottom image represents the mesh used for the blade span.

tation, implicit discretization using double precision was retained, as indicated the high scale differences between the geometric details of the modeled turbine stage. Initially, the computations used a first-order discretization in space. Later, these were toggled to the second order accuracy.

For this test case, three meshes of diverse density were produced to take into account grid independence. Results obtained via mesh A with 224,136 nodes and mesh B with 610,067 nodes presented only minor discrepancies, mainly visible at the stator trailing edge due to the occurrence of a supersonic bubble in that region. In order to improve computational efficiency, the intermediate mesh C comprising 395,296 nodes was used to obtain the following results.

The flowfield at inlet to the stator was fully subsonic. Transonic flow was restricted to the minor zones around the stator trailing edge. Thus, at the stage inlet, we imposed stagnation pressure and temperature with their corresponding flow angles. Meanwhile, at the stage outlet, static pressure was imposed. At the mixing-plane interface, the characteristic boundary conditions were imposed. These correspond to stagnation pressure, temperature, and flow angles at the rotor inlet and static pressure at stator outlet. In the application of the SA turbulence model, we set a turbulence intensity of 10% and a length scale of 1% pitch at stator mid-span. These turbulence values are typical for modern low-pressure turbine stages. Although the separation points were well predicted, the size of the separation was extremely dependent on length scale. Incidentally, its real value was not provided by the experiments.

Initial computations were performed explicitly using pure characteristic boundary conditions to extrapolate the variables at the boundaries. Unfortunatelly, convergence was not attained; the residues stucked at a minor value. Convergence was attained only when an implicit formulation that applies non-reflecting boundary conditions was used.

Due to computing power restrictions, only the results for the SA turbulence model using wall functions were obtained. Fig. 8 presents the numerical results obtained for the velocity distribution at a section in stator mid-span. These could be compared with the experimental results obtained for the stage using particle image velocimetry (PIV). Experimental results were obtained in two windows, the first located between the stator and rotor, and the second after the rotor. These windows are illustrated in Fig. 8(a) to allow for easier comparison between numerical and experimental results.

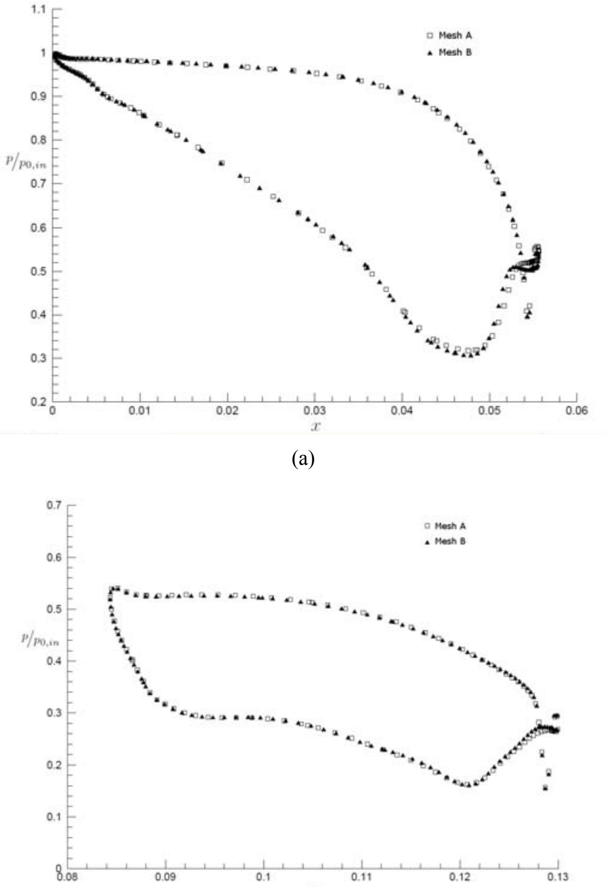

(a)

(b)

Fig. 7. Pressure ratio distribution for the results obtained via mesh A with 224,136 nodes and with mesh B with 610,067 nodes. (a) Results obtained at stator mid-span; (b) results obtained at rotor mid-span.

The numerical results showed good agreement with experimental data. However, the values following the stator exit were much better predicted by the numerical model. Thus, caution should be exercised when comparing exit stator results. The definition of a mixing plane implies averaging, which makes it impossible to compare the numerical and experimental results effectively in that region, at least in the part of the windows that follows the mixing-plane.

Additional experimental data are necessary for a precise validation of the model. Only with a spanwise distribution of experimental and computed variables could the capability of the mixing plane model in the prediction of this flowfield be assessed fully.

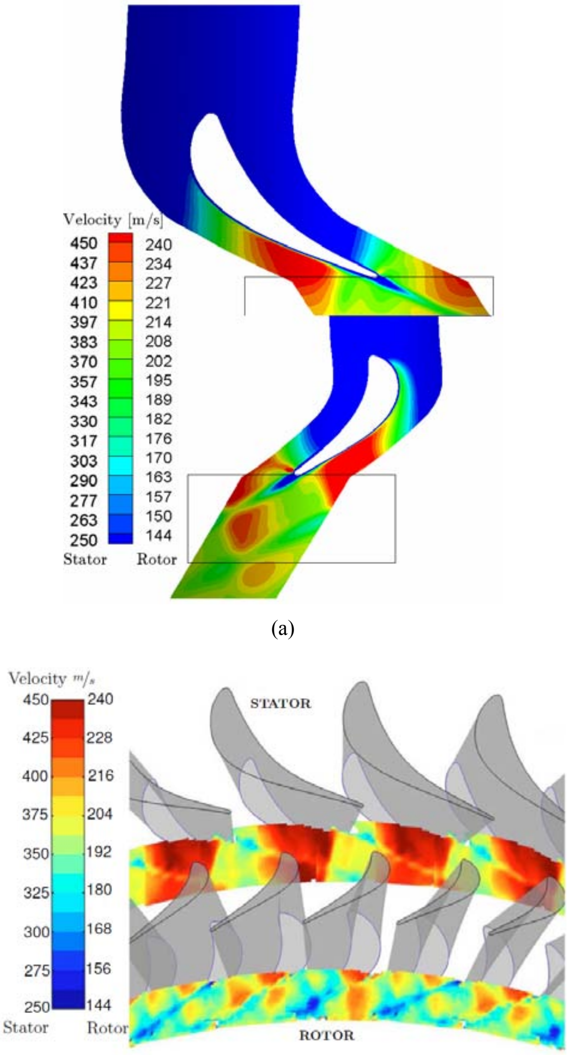

(a)

(b)

Fig. 8. Results obtained for the computation of the Graz transonic turbine stage: (a) isolines of velocity for a circumferential section at stator mid-span (r=0.226) computed using the mixing-plane approach; (b) experimental results obtained using PIV at Technical University of Graz.

However, results were not available for the pressure distribution on the blades. But Mach number results were readily available from a traverse radial plane located immediately after the stator blade row. This plane was defined at 0.026 mm from the stator blade leading edge. Fig. 9 depicts the results of the numerical computations compared with experiments. For clarity, two blade pitches were presented. These results were obtained without computing the full boundary layer and by resorting to wall functions. Based on the results presented for the T106 cascade, it was expected that secondary flows would be under-predicted. The mixing plane approach was applied, and thus, the resolution of the full wall boundary would be counterproductive, as it would be influenced by the averaging approach.

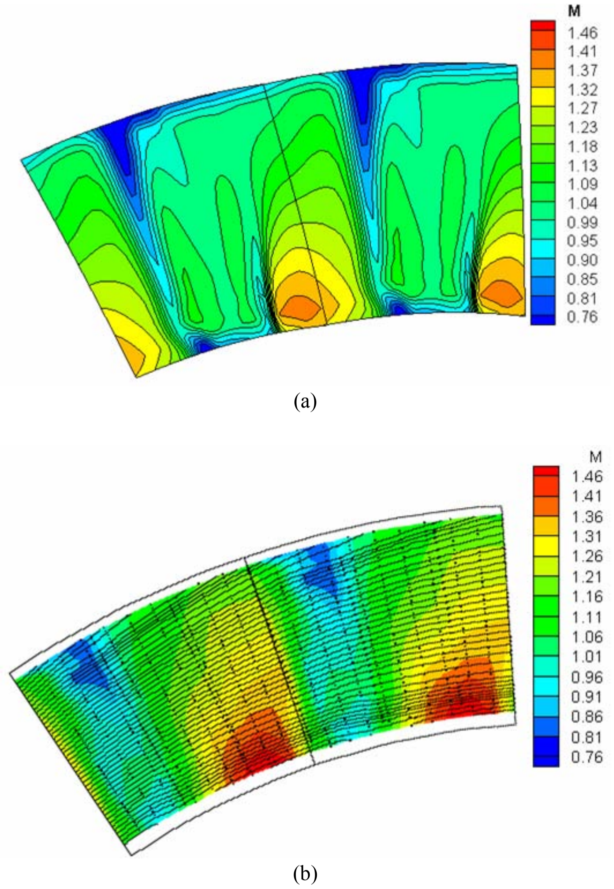

(a)

(b)

Fig. 9. Results obtained for the computation of the Graz transonic turbine stage: (a) isolines of a Mach number in a radial plane immediately after the stator trailing edge (0.026 mm from the leading edge of the blade) computed using the mixing-plane approach; (b) experimental results obtained using a pressure probe at the Technical University of Graz.

3. Conclusions

A study on accuracy limitations related to the computation of turbulent flow in gas turbines was performed. Accuracy was partly limited by the expensive computing resources needed to model the complex geometries involved, and by the accuracy of the available physical models.

Detailed flow analysis was performed as well for a rectilinear cascade involving secondary flow representation. Results clearly showed that only low Reynolds number models resolving the full boundary layer could approach the level of experimental results. Nevertheless, the modeling of secondary flows in these regions could be still computed through approximations, and even by solving for the full boundary layer.

The latter implies that low Reynolds number turbulence models should be employed in computing stage flows. Nevertheless, we noted some problems existing with the computation of the transonic stage. Although first order convergence was attained readily, second order computations were difficult to obtain for the refined meshes. These difficulties could compromise the results even at the level of accuracy already obtained via the wall functions. Thus, whether the use of a fully resolved boundary layer when using a mixing-plane approach is beneficial or not is the question that needs to be addressed.

Studies on turbulence modeling of compressible flow using the mixing plane algorithm implemented in FLUENT® are scarce in existent literature. The references mainly focus on incompressible flow applications. If we restrict our research to simulations that present supersonic pockets near the mixing plane interface, available references would be almost non-existent; meanwhile, to the best of our knowledge, available publications do not go beyond first-order discretization convergence [13]. In the present work, we presented a second order computation for this class of flow [14, 15] that deal with the formation of supersonic pockets due to the thickness of stator trailing edge impinging on the mixing plane and causing convergence problems.

By referring to the mixing plane models, we could deduce that the flow mixes almost instantaneously into a pitchwise uniform flow. This mixing could cause an overestimation of losses, similar to a real machine wherein the mixing process is partly achieved through the rotor itself. Even with this modeling assumption, the difference between the computed losses using the mixing-plane and an unsteady computation is not highly significant.

Acknowledgment

This work was partly supported by Center for Aerospace Science and Technology (CAST), FCT Research Unit Nº151.

Nomenclature

c : Blade chord
c_{ax} : Axial chord
p : Static pressure
$p_{0,in}$: Inlet stagnation pressure
PS : Pressure surface
s : Pitch
SS : Suction surface

References

[1] U. Köller, R. Mönig, B. Küsters and H-A. Schreiber, Development of advanced compressor airfoils for heavy-duty gas turbines – Part 1: design and optimization, *Journal of Turbomachinery*, 122 (2006) 397-405.

[2] J. C. Páscoa, J. K. Luff, J. J. McGuirk and A. C. Mendes, On accurate numerical modeling of 3D turbulent flow through a DCA compressor cascade and its experimental validation, *International Journal of Dynamics of Fluids*, 2 (1) (2006) 1-18.

[3] S-B. Kwon, S-J Lee, S-Y Shin and S-H Kim, A study on the flow with nonequilibrium condensation in a minimum length nozzle, *Journal of Mechanical Science and Technology*, 23 (2009) 1736-1742.

[4] C. H. Sohn and H. C. Cho, A CFD study on thermo-acoustic instability of methane/air flames in gas turbine combustor, *Journal of Mechanical Science and Technology*, 19 (9) (2005) 1811-1820.

[5] J. D. Denton, The calculation of three-dimensional viscous flow through multistage turbomachines, *Journal of Turbomachinery*, 114 (1992) 18-26.

[6] J. C. Páscoa, A. C. Mendes and L. M. C. Gato, A fast iterative inverse method for turbomachinery blade design, *Mechanical Research Communications*, 36 (5) (2009) 630-637.

[7] J. C. Páscoa, A. C. Mendes and L. M. C. Gato, Aerodynamic design of turbomachinery cascades using an enhanced time-marching finite volume method, *CMES – Computer Modeling in Engineering & Sciences*, 6 (6) (2004) 537-546.

[8] B. Koobus, S. Camarri, M. V. Salvetti, S. Wornom and A. Dervieux, Parallel simulation of three-dimensional complex flows: Application to two-phase compressible flows and turbulent wakes, *Advances in Engineering Software*, 38 (5) (2007) 328-337.

[9] Y. Liu, Aerodynamics and heat transfer predictions in a highly loaded turbine blade, *International Journal of Heat and Fluid Flow*, 28 (2007) 932-937.

[10] S. Djouimaa, L. Messaoudi and P. W. Giel, Transonic turbine blade loading calculations using different turbulence models – effects of reflecting and non-reflecting boundary conditions, *Applied Thermal Engineering*, 27 (2007) 779-787.

[11] E. Göttlich, J. Woisetschläger, P. Pieringer, B. Hampel and F. Heitmeir, Investigation of vortex shedding and wake-wake interaction in a transonic turbine stage using laser-doppler-velocimetry and particle-image-velocimetry, *Journal of Turbomachinery*, 128 (2006) 178-187.

[12] L. Cutrone, P. D. Palma, G. Pascazio and M. Napolitano, Predicting transition in two and three-dimensional separated flows, *International Journal of Heat and Fluid Flow*, 29 (2008) 504-526.

[13] D. Hanus, T. Censký, J. Neveceral and V. Horký, First stage of the centrifugal compressor design with tandem rotor blade, *Proc. ISABE – 17th International Symposium on Air-breathing Engines, Munich, Germany (2005) ISABE-2005-1161.*

[14] C. Xisto, *Estudo da Física do Escoamento Secundárioe Modelação do Escoamento Turbulento 3D em Coroas de Pás de Turbinas*, Dissertation (in Portuguese), University of Beira Interior, Covilhã, Portugal (2009).

[15] G. Kalitzin, G. Medic, G. Iaccarino and P. Durbin, Near-wall behavior of RANS turbulence models and implications for wall functions, *Journal of Computational Physics*, 204 (2005) 265-291.